Case Studies in Thermal Engineering 50 (2023) 103399

Contents lists available at ScienceDirect

Case Studies in Thermal Engineering

journal homepage: www.elsevier.com/locate/csite

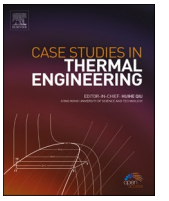

Effects of Initial Temperature, Initial Pressure, and External Heat Flux on the Thermal Behavior of Ethanol/Biodiesel as Biomass Structures

Gongxing Yan [a,b], Omar S. Mahdy [c], As'ad Alizadeh [d,**], Navid Nasajpour-Esfahani [e], Shadi Esmaeili [f], Maboud Hekmatifar [g,*], Mohamed R. El-Sharkawy [h], Ahmed Salah Al-Shat [i], Mahmoud Shamsborhan [j]

[a] *School of Intelligent Construction, Luzhou Vocational and Technical College, Luzhou, 646000, Sichuan, China*
[b] *Luzhou Key Laboratory of Intelligent Construction and Low-carbon Technology, Luzhou, 646000, Sichuan, China*
[c] *Department of Chemical Engineering, University of Technology, 52 Alsinaa St., P.O. Box 35010, Baghdad, Iraq*
[d] *Department of Civil Engineering, College of Engineering, Cihan University-Erbil, Erbil, Iraq*
[e] *Department of Material Science and Engineering, Georgia Institute of Technology, Atlanta, 30332, USA*
[f] *Faculty of Physics, Semnan University, P.O. Box: 35195-363, Semnan, Iran*
[g] *Department of Mechanical Engineering, Khomeinishahr Branch, Islamic Azad University, Khomeinishahr, Khomeinishahr, Iran*
[h] *Al-Amarah University College, Engineering of Technical Mechanical Power Department, Maysan, Iraq*
[i] *Al-Mustaqbal Universty, College of Engineering and engineering Technologies, Chemical Engineering and Oil Industries Department, 51001, Babylon, Iraq*
[j] *Department of Mechanical Engineering, College of Engineering, University of Zakho, Zakho, Iraq*

* Corresponding author.
** Corresponding Author
E-mail addresses: yaaangx@126.com (G. Yan), asad.alizadeh2010@gmail.com (A. Alizadeh), Maboud.Hekmatifar@iaukhsh.ac.ir (M. Hekmatifar).

https://doi.org/10.1016/j.csite.2023.103399

Available online 21 August 2023

G R A P H I C A L A B S T R A C T

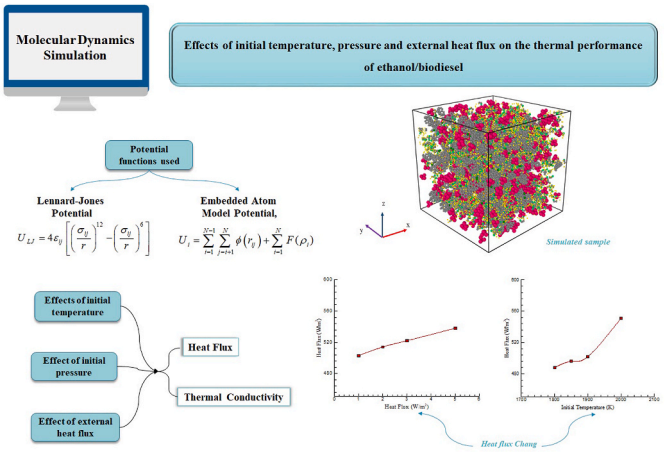

A R T I C L E I N F O

Handling Editor: Huihe Qiu

Keywords:
Biomass
Biodiesel
Temperature
Pressure
Molecular dynamics simulation

A B S T R A C T

The emergence of significant environmental problems, the depletion of fossil fuel reserves, and the anticipation of price hikes have driven researchers to explore and adopt renewable fuels derived from biological sources. Such renewable energy sources include biomass, biodiesel (BD), ethanol, bioethanol (BE), among others. Biomass is a form of energy that can be obtained from waste or the cultivation of specific plants. Notably, BD fuel can be produced from organic sources, such as animal fats or waste oil from restaurants, which is a considerable advantage of BD. Moreover, BE is a non-toxic, safe, and biodegradable fuel, and ethanol produced biologically is referred to as BE, which represents a renewable fuel with a non-fossil origin. Against this backdrop, the upcoming research employs two types of alcoholic fuel, ethanol and BD, as biomass structures. Using molecular dynamics (MD) simulation, the study evaluated the effects of temperature (Temp), pressure (Press), and external heat flux (EHF) on thermal parameters, such as HF and thermal conductivity (TC). The evaluation results indicated that an increase in the initial temperature from 1800 to 2000 K led to higher mobility of the samples, resulting in an increase in the values of HF and TC from 488 to 551 W/m^2 and 0.26–0.32 W/m.K, respectively. Similarly, raising the initial Press from 1 to 5 bar increased the number of oscillations and mobility of the structures, leading to increased HF and TC values from 488 to 551 W/m^2 and 0.26–0.32 W/m.K, respectively. Notably, the EHF changes exhibited similar behavior. Additionally, a significant outcome was observed when the EHF rose from 1 to 5 W/m^2. This increase in EHF led to a corresponding rise in the number of reactions occurring in the studied structure. As a result, the released heat intensified, leading to increased HF and TC values. Specifically, HF values rose from 503 to 538 W/m^2, and TC increases from 0.28 to 0.31 W/m.K.

1. Introduction

Similar to how petroleum was processed in a refinery to produce fuel, plastics, and chemical-petroleum compounds, a biorefinery used agricultural raw materials, secondary products, and bio-wastes to create a range of products, including food compounds, pharmaceutical compounds, and biofuels. However, many biomass-derived fuels were economically feasible only when a valuable by-product can be recycled during processing and efficient energy control was used. Biomass was the oldest source of energy for humans, and this energy-carrying product stores the sun's energy continuously (renewable) and can be converted directly or indirectly into liquid fuels [1–3]. Biomass can be converted into various forms of fuel, such as alcohol-based fuels and BD, which were suitable substitutes for gasoline, gaseous fuels like biogas and bio-hydrogen (H_2), or solid fuel, such as burning wood. Hence, there was a high diversity in production, storage, and consumption [4,5]. Additionally, biomass can be utilized to generate electrical energy, either directly or indirectly. The derivatization of biomass into biofuel can be achieved using both edible and non-edible biomass. Some biofuels, such as oil extracted from plants and algae, were a direct product of photosynthesis. Some, such as ethanol produced by yeasts and bacteria, result from biomass derivatization and conversion, and others, like H_2, can be produced both ways [3]. Ethanol, or ethyl alcohol, was one of the promising alternative sources of fossil fuels that received much attention [6–8]. This substance is one of the

most common alcohols. It can be easily produced during the fermentation of grains (starch), fruit juices, and any other source that can provide sugar to the fermenting microorganism [9–12]. Ethanol, also known as the "fuel of the future" according to Henry Ford, emerged as the most commonly used alcoholic fuel due to several factors. Compared to other alcohols, its toxicity was lower, and the secondary products resulting from the incomplete oxidation of ethanol, such as acetic acid and acetaldehyde, were less toxic than those resulting from other alcohols. Additionally, ethanol dissolves in water at any concentration and can be produced from renewable agricultural products, such as sugar, corn, lignocellulose, among others. This made it a more sustainable option compared to non-renewable petroleum products. The significance of utilizing ethanol and biodiesel as biomass stems from their potential as renewable and eco-friendly biofuels that decrease greenhouse gas emissions and enhance energy security. Furthermore, exploring the thermal properties of diesel, ethanol, biodiesel, zero-carbon fuel and other fuels was crucial for optimizing combustion processes, comprehending their performance under diverse conditions, and ensuring their efficient utilization across various applications [13–16].

Exploration in this field facilitated the advancement of biofuels with reduced carbon footprint and supported the worldwide shift towards cleaner and more sustainable energy alternatives. Various experimental and simulation techniques, such as molecular dynamics (MD) and machine learning (ML), were used to study the thermal behavior of ethanol and biodiesel as biomass. The following section highlights some of these approaches. Do et al. [17] conducted a thorough investigation into the effect of external heating flux (EHF) and different initial temperatures (Temps) in the presence of a 10% platinum nanocatalyst on various combustion process-related parameters. The study revealed interesting trends in the number of H2 molecules across different temperature ranges, with higher EHF leading to a downward trend and a decrease in H_2 molecules from 603 to 589. Meanwhile, Falani Ozbas et al. [18] offered valuable insights into H_2 production from biomass gas conversion. This study used supervised machine learning algorithms and proposed model structures as a sturdy approach for precise H_2 concentration prediction. The research results contribute to the advancement of H_2 production technologies, which played a crucial role in sustainable energy and environmental conservation. Zhang et al. [19] conducted a comprehensive investigation into the effect of temperature on the biomass gasification process using MD simulation. The researchers aimed to comprehend the effect of various temperatures on chemical reactions and gas production during biomass gasification. The research findings suggest that significant changes occur in the gasification process with increasing temperature. Notably, higher temperatures result in increased production of H_2 and hydroxide radicals (OH). These reactive species played a crucial role in gasification reactions and contribute to overall gas production. In particular, elevated temperatures led to an increase in the production of CO and H_2. This implies that higher temperatures promoted the decomposition of biomass molecules and yielded higher amounts of CO and H_2 gases. Esawi et al. [20] analyzed the effect of biodiesel (BD) fuel on ethanol/diesel blends. The research findings revealed that a blend of 15% BD, 5% ethanol, and 80% diesel fuel caused minor changes in droplet lifetime, cetane number (CN), viscosity, and calorific value of pure diesel, with less than 1.2 %, 0.2 %, and 2 %, and 2.2 % reduction in the mentioned values, respectively. Meanwhile, Celebi et al. [21] investigated the effects of adding butanol to safflower BD fuel consumption in a diesel engine. The butanol-BD blends and diesel-BD-butanol blends contained 5 %, 10 %, and 20 % butanol by volume. Qi et al. [22] examined the effect of adding methanol to BD-diesel blends on a diesel engine's combustion characteristics and engine treatment. The base fuel used in their research was BD50, which contains 50 % BD. Methanol was incorporated into BD50 as an additive at volume percentages of 5 % (BDM5) and 10 % (BDM10). Meanwhile, An et al. [23] investigated the combustion treatment and emission attributes of a diesel engine using BD fuel under partial load conditions. The research findings demonstrated that BD fuels had a significant effect on brake thermal efficiency (TE).

This research mainly focused on understanding the effect of factors, such as temperature, Press, and EHF on important thermal parameters, including HF and thermal conductivity (TC) in the presence of 10% platinum catalyst. Platinum's exceptional catalytic activity, stability, compatibility with biomass structures, nanoscale properties, and versatility made it an excellent choice for simulation research aimed at comprehending the thermal behavior and reactivity of ethanol and biodiesel as promising biomass-based fuels. To achieve this, advanced MD simulations were used, providing a detailed and atomistic understanding of the underlying phenomena. The findings obtained from the simulation of the fundamental structure of biomass in this study can be highly useful in assessing the experimental conversion of biomass to gas. While these two methods of simulation and experimentation differ in approach, they complement each other, and combining them can offer a unique perspective on the behavior of biomass during the conversion process. Therefore, the combination of simulation and experimental techniques can serve as a valuable tool in evaluating experimental biomass-to-gas conversion and enable researchers to make informed decisions for practical applications in the field of biomass conversion. At first, the researchers focused on assessing the intricate interplay of changes in critical physical parameters, such as kinetic energy (KE) and thermal energy (TE), within the target structures over a 2 ns timescale. This duration was selected to ensure the collection of meaningful data, capturing the dynamic behavior of the system being studied. Subsequently, the investigation delved into a more thorough analysis of heat treatment. This involved a systematic exploration of the effects induced by various temperature values, Press conditions, EHF, HF within the system, and the TC of the materials. The objective here was to elucidate the thermal behavior and intricate molecular-level interactions occurring under various experimental conditions. Through this comprehensive study, the researchers aimed to facilitate a deeper understanding of the thermal properties and behavior of the selected biomass structures under different external influences. The findings of this research are expected to contribute significantly to advancing renewable energy applications, and further optimize the utilization of alcoholic fuels in energy production and conservation.

2. The MD simulation approach

Computer simulation is a highly effective approach for studying material treatment. The primary goal of MD simulation is to compute the macroscopic behavior of a system using a microscopic model that incorporates interactions among particles. By analyzing

the behavior of these components, macroscopic and microscopic quantities can be obtained. Since molecular systems typically comprise numerous particles, it is impractical to determine the attributes of complex structures analytically. Therefore, the MD simulation untangles this issue by utilizing computational procedures. The basic equation on which the MD method was developed is expressed using following equation [19,24,25]:

$$F_i = m_i a_i = -\nabla_i U = -\frac{dU}{dr_i} \tag{1}$$

$$a_i = \frac{d^2 r_i}{dt^2} \tag{2}$$

Using the equations given above, an equation that calculated the position of the particles in terms of the potential function was obtained:

$$-\frac{dU}{dr_i} = m_i \frac{d^2 r_i}{dt^2} \tag{3}$$

In MD simulation, Eq. (3) is utilized to solve various problems, where the force on particles depends on their relative positions to each other. Analytically solving these problems involved numerous complexities; hence, numerical methods were used to address them. Using this integral, the total force applied to each particle in the configuration at time t was computed as the sum of its interactions with other particles. Moreover, the particle acceleration was calculated from the resultant forces applied to each particle. The formulation of this method is as follows [26,27]*:*

$$r_i\,(\mathrm{t}+\Delta\mathrm{t}) = 2\,r_i(t) - r_i(t-\Delta t) + \left(\frac{d^2 r_i}{dt^2}\right)(\Delta t)^2 \tag{4}$$

$$v_i(t+\Delta t) = v_i(t) + \Delta t\; v_i(t) + \frac{\Delta t\,(a_i\,(t) + a_i(t+\Delta t))}{2} \tag{5}$$

The designation of the potential function and interparticle forces was a crucial parameter in MD simulation. In conventional MD simulation, interatomic interactions were defined using a force field. The potential energy of a system comprising particles was computed using the potential and interparticle force functions in MD simulation. Therefore, their precise selection was critical, and various researchers developed their own types. Lennard Jones (LJ), EAM, and Coulomb's potential functions were used for the interaction among particles in the simulation of biomass structure [28–30]. The most common potential used in a computer simulation was the LJ potential. In non-bonded interactions, all pairs of particles i and j that were located at a ridge distance from each other interact with each other in terms of LJ force, which is obtained as follows [31]:

$$\mathrm{U_{LJ}} = 4\varepsilon_{\mathrm{ij}}\left[\left(\frac{\sigma_{\mathrm{ij}}}{\mathrm{r_{ij}}}\right)^{12} - \left(\frac{\sigma_{\mathrm{ij}}}{\mathrm{r_{ij}}}\right)^{6}\right], \mathrm{r_{ij}} < \mathrm{r_c} \tag{6}$$

Using the data given in Table 1, as well as Eqs. (7) and (8), the values of σ and ε of each of reactions among the particles are calculated as follows [32–34]:

$$\varepsilon_{ij} = \sqrt{\varepsilon_i \varepsilon_j} \tag{7}$$

$$\sigma_{ij} = \frac{\sigma_i + \sigma_j}{2} \tag{8}$$

EAM potential function described the reactions among metal particles of matrix, expressed by the following equations [28].

$$U_i = \sum_{i=1}^{N-1} \sum_{j=i+1}^{N} \varphi(r_{ij}) + \sum_{i=1}^{N} F(\rho_i) \tag{9}$$

$$\rho_i = \sum_{i=1}^{N} \psi(r_{ij}) \tag{10}$$

Table 1
LJ potential parameters of present particles [31,32].

Atom	ε_{ij} (kcal/mol)	σ_{ij} (Å)
H	0.044	2.886
O	0.06	3.500
Pt	0.080	2.754
Cl	0.227	3.947
C	0.105	3.851

where i and j are the atoms present in the interaction process among N atoms with the distance r_{ij}. $\Phi(r_{ij})$ represents the interatomic energy, and F (ρ_i) is the potential embedding function. Finally, the electrostatic potential energy is obtained from the constant Coulomb forces [30]:

$$U_{ij}(r) = \frac{-1}{4\pi\varepsilon_0}\frac{q_i q_j}{{r_{ij}}^2} \tag{11}$$

It is worth noting that r_{ij} in interatomic potential functions, such as embedded atom method (EAM) and Coulomb potential indicates the distance between two atoms i and j in a polyatomic system. However, the physical meaning, and mathematical expressions in these potentials differed in terms of the nature of interactions they described. r_{ij} in the EAM potential represents the interatomic distance between two atoms in a metal system, which calculated short-range repulsive and long-range embedded interactions among atoms. But, in Coulomb potential, r_{ij} represents the distance between two charged particles, usually ions or point charges, and described the Coulomb potential, known as the electrostatic potential.

2.1. Simulation details in the current study

This study uses MD simulation to investigate the effect of EHF, initial temperature, and initial pressure (Press) on the thermal properties of a biomass structure comprising ethanol/BD. Initially, the biomass structure was situated in a simulation box with dimensions of 100 × 100 × 100 $Å^3$. The particle structure was modeled separately using Avogadro software and then simulated using LAMMPS software. The reaction temperature for simulation was adjusted at 1800 K utilizing a Nose-Hoover thermostat. The changes in KE and total energy (TE) were evaluated to check the balance in the simulated structure. Then, to create the combustion process and reach the T=1800 K, considered ensemble was changed from NVT to NPT. The effects of initial temperature changes (1800, 1850, 1900, and 2000 K), initial Press changes (1, 2, 3, and 5 bar), as well as EHF (1, 2, 3, and 5 W/m^2) on thermal parameters such as HF, TC, was studied using the MD simulation and LAMMPS software. Fig. 1 illustrates the overview of atomic structure containing ethanol, BD, oxygen, H_2, and CO samples inside the simulation box at the EHF of 1 and 5 W/m^2 and T=1800 K.

3. Results and discussion

At the beginning of this section, the equilibrium of simulated atomic sample, including the simulated sample, was verified. This sample was equilibrated under standard conditions. Subsequently, thermal quantities, including HF and TC, were examined to assess the reaction and thermal treatment of the structure.

3.1. Equilibrium process

In this section, the chnages in physical components, such as kinetic energy (KE) and thermal energy (TE), of the simulated structure were examined to ensure its stability. The changes in KE after 2 ns are illustrated in Fig. 2, and it is evident that KE converged to 72.89 eV. All particles in the simulation box oscillated using the suitable potential to the structure under study. In the early times, the fluctuations were more, and over time the particles are coupled with the applied potential function, and the particles were placed in the right place. Because of this, fluctuations were reduced, and balance was established in the system. Therefore, with the convergence of KE, the temperature of the atomic structure approached. The observed KE changes and the KE convergence to a certain number indicated the reliable choice of atomic structures and interatomic potential.

The convergence of TE to −7002.204 eV in desired structure after 2 ns can be seen in the obtained results (See Fig. 3). The negative TE means the gravitational energy exceeds the atomic vibrational motions. When the energy of attraction among the particles was higher, the particles were closer to each other, and the oscillations were reduced, which led to the stability of the whole structure under study.

3.2. The initial temperature effect on the thermal treatment of the desired structure

The initial temperature plays a significant role in driving the desired structural evolution. At the atomic level, an increase in

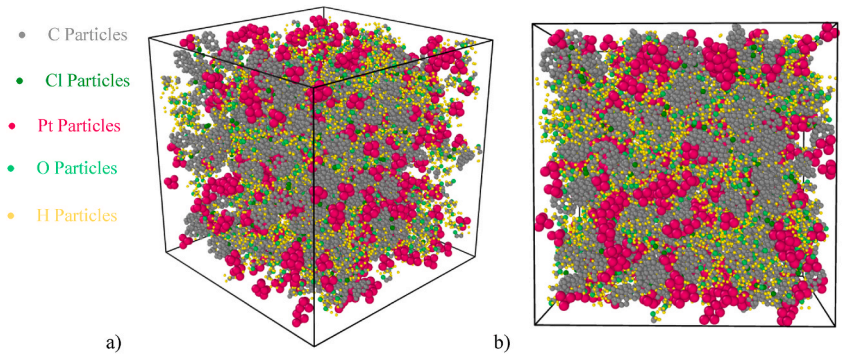

Fig. 1. Atomic arrangement of the simulated sample from a) perspective and b) side view.

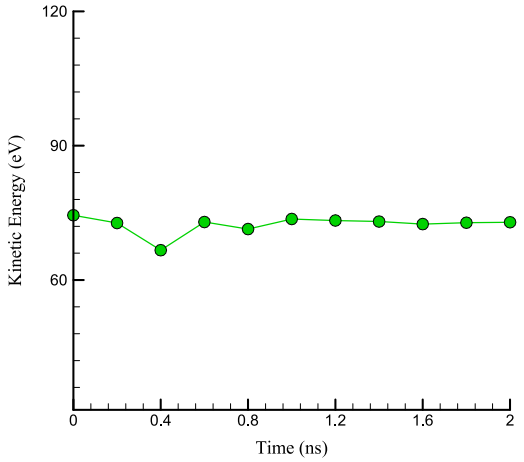

Fig. 2. The changes of KE of simulated atomic samples during 2 ns.

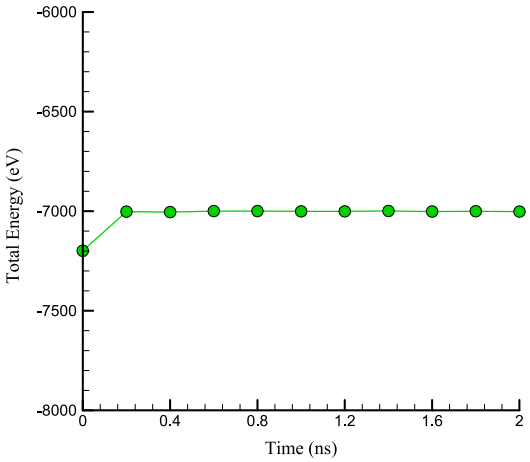

Fig. 3. The changes of TE of simulated atomic samples during 2 ns.

temperature led to enhanced mobility in the samples, ultimately resulting in higher kinetic energy (KE) and thermal energy (TE) values [35,36]. To examine the effect of initial temperature on the thermal behaviour of studied samples, T=1800, 1850, 1900, and 2000 K were selected. In this section, the changes of HF and TC based on the increase in the initial temperature of the samples were studied. The increase in temperature in the structures corresponding to the atomic transformation was more intense, and more HF is expected from the samples. Furthermore, with the initial temperature increasing from 1800 to 2000 K, the HF inside the structure increases from 260 to 551 W/m$^{2.}$(See Fig. 4).

An increase in the HF of the samples led to an increase in the TC in the atomic structure. Also, the increase in HF led to a decrease in the energy of interatomic attraction and an increase in the oscillation range of the samples (See Fig. 5).

The numerical results of changes in HF and TC for initial temperature changes in ethanol/BD structure and in the presence of 10% platinum nanocatalyst are presented in Table 2.

In general, increasing the initial temperature in atomic structures resulted in higher HF due to the increased kinetic energy, vibrational motion, and accelerated diffusion. Additionally, elevating the initial temperature in atomic structures led to greater phonon transport, longer mean free paths, increased phonon-phonon interactions, faster energy release, higher vibrational frequencies, and thermally activated carriers. These physical mechanisms collectively contributed to observed increase in TC, allowing materials to conduct heat more effectively by increasing temperature. This physical behavior was essential for understanding HT and thermal properties in various materials and played an important role in applications. It played different roles, from material science to energy systems (see Fig. 5).

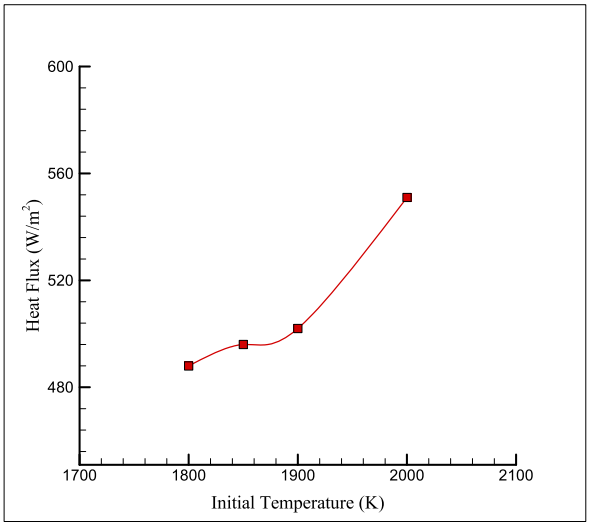

Fig. 4. The changes in HF per initial temperature for 10% platinum catalyst.

Table 2
The results of the performed simulation at different initial temperature.

Initial temperature (K)	HF (W/m^2)	TC (W/m.K)
1800	488	0.26
1850	496	0.28
1900	502	0.31
2000	551	0.32

3.3. The effect of initial press on the thermal treatment of the desired structure

To investigate the effect of initial Press on the thermal treatment of the models, initial Press of 1, 2, 3, and 5 bars were considered. Fig. 6 illustrates the changes in heat flux (HF) of the simulated samples as the initial Press increased. Elevating the initial Press in the desired structures increased the number of oscillations and, consequently, the mobility of structures. Therefore, an increase in initial Press is expected to lead to higher HF values. In other words, the number of reactions in the structure increased in terms of the lowering of activation energy. Consequently, reducing the distance among atoms in the simulated samples was a more important factor than the mobility of atoms. As a result, chemical reactions with higher intensity were observed by increasing Press. This caused an increase in the HF flowing in studied structure. Atomically, by increasing the Press in the desired structure to 5 bar, the HF increases to 496 W/m^2.

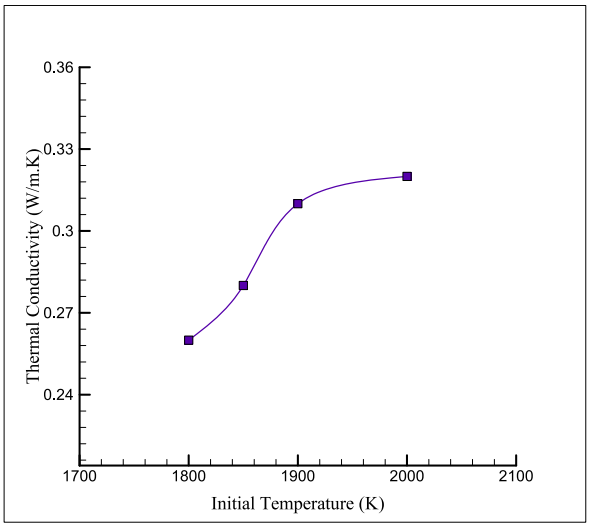

Fig. 5. The changes in TC per initial temperature in the presence of 10 % platinum catalyst.

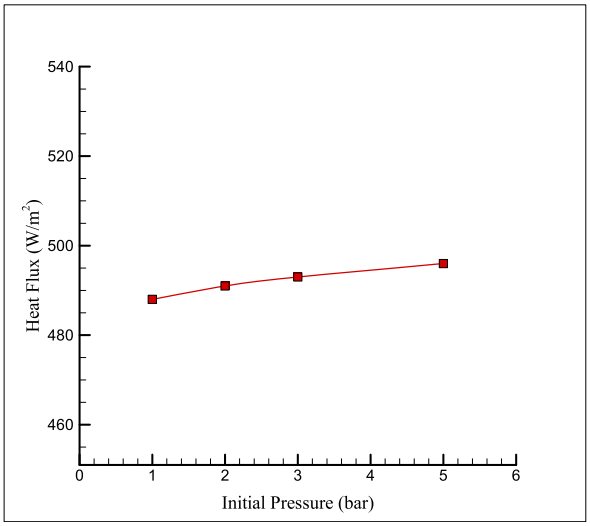

Fig. 6. The changes in HF per initial Press with 10% platinum catalyst.

As mentioned before, by increasing initial Press, the mobility of atoms increases, and consequently, chemical reactions with higher intensity were observed. Atomically, by increasing the Press in the structures to 5 bar, the TC of the samples increases to 0.28 W/m.K. The outcomes illustrate that, at P = 1, 3, and 5 bar, the values of TC equal to 0.26, 0.27, and 0.28 W/m.K, respectively (See Fig. 7).

The numerical results of changes in HF and TC for initial Press changes in ethanol/BD structure and in the presence of 10% platinum nanocatalyst are listed in Table 3.

In general, increasing the initial Press in atomic structures led to a higher frequency of atomic collisions, which increased particle density and improves energy transfer paths, vibrational motion, and diffusion (see Table 4). These physical mechanisms collectively enhanced heat flux (HF) and enabled materials to conduct heat more efficiently at higher Press. Conversely, increasing the initial Press in atomic structures led to increased phonon transport, which reduced mean free paths. Elevating the initial Press in atomic structures increased particle density, altered network dynamics, created new energy transfer pathways, accelerated diffusion, and led to faster attainment of thermodynamic equilibrium. These physical mechanisms collectively contributed to the observed increase in TC, enabling the material to conduct heat more efficiently as Press increases. Understanding these behaviors was crucial for various applications, including materials science, thermodynamics, and high-temperature engineering.

3.4. The effect of EHF on the thermal treatment of the desired structure

In the final part of this research, the effect of EHF on the thermal treatment of ethanol, BD, oxygen, hydrogen, and CO samples simulated was studied. Therefore, HF in the models was considered equal to 1, 2, 3, and 5 W/m^2. Fig. 8 illustrates the changes in the HF in terms of the increase in the EHF applied to the atomic models. Increasing the number of reactions created caused an increase in the heat released in the defined samples. According to the obtained results , HF increases to 538 W/m^2 after 2 ns and using the initial heat flux with the intensity of 5 W/m^2.

Fig. 9 illustrates the changes in TC obtained by increasing the EHF applied to the desired models. Therefore, the heat released in the defined models increased. According to the results obtained in this part, the TC value of the samples increased to 0.31 W/m.K after 2 ns and using the initial HF with an intensity of 5 W/m^2. The numerical results showed that in the HF applied with 1, 2, 3, and 5 W/m^2 values, the TC in the samples reached the values of 0.28, 0.28, 0.29, and 0.31 W/m.K.

Elevating EHF generally provided additional thermal energy to the atomic structure, leading to increased phonon transport, accelerated vibrational motion, higher temperature gradients, increased TC, and faster, more efficient diffusion. These physical mechanisms collectively enhanced heat flux (HF) and enabled materials to conduct heat more efficiently as EHF increased. On the other hand, the increase of EHF did not change the TC atomic structures by itself. Instead, it affected the rate of HT and temperature distribution within the material, which may lead to temperature-dependent effects that should be considered when studying thermal behavior. TC remains a constant material property that characterized the ability of materials to conduct heat under certain conditions. Understanding these behaviors was important for applications, including HT engineering, material processing, and thermal management systems. Finally, it was determined that the results obtained from this study could correctly explain the studied sample's thermal behavior under different temperatures, Press, and EHF conditions. These findings provided valuable insights into the dynamic properties of energy and HT, enabling a better understanding of thermal response of materials, and their potential applications in relevant industries.

4. Conclusion

Biomass is one of the types of energy that can be obtained from waste or the cultivation of special plants. Production of BD fuel from

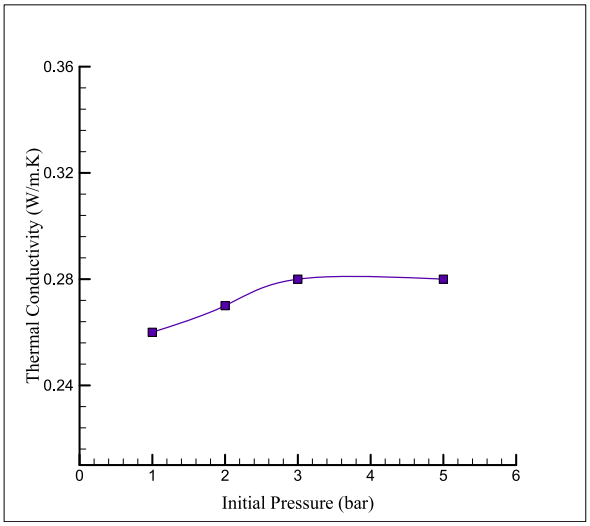

Fig. 7. The changes in TC per initial Press.

Table 3
The results of the performed simulation at a different initial Press.

Initial Press (bar)	HF (W/m^2)	TC (W/m.K)
1	488	0.26
2	491	0.27
3	493	0.28
5	496	0.28

Table 4
The results of the performed simulation at a different initial Press.

EHF (W/m^2)	HF (W/m^2)	TC (W/m.K)
1	503	0.28
2	514	0.28
3	522	0.29
5	538	0.31

organic sources, such as vegetable oils, animal fats, or waste oil from restaurants was the main advantage of BD. BE was a non-toxic, safe, and biodegradable fuel. Ethanol that was produced biologically is called BE, which was a renewable fuel with a non-fossil source. The effects of temperature, Press, and EHF on thermal parameters such as HF and TC were evaluated using the MD simulation. At first, the balance of changes in physical parameters, such as KE and the TE of desired structure was studied after 2 ns. Then, to analyze the thermal treatment, the effects of the quantities of temperature, Press, and EHF on HF and TC were studied. The results are as follows:

- The studied structure reached thermal equilibrium after 2 ns, and the value of KE and TE in this structure approached 72.89 and −7002.204 eV, respectively.
- An increase in temperature from 1800 K to 2000 K led to a corresponding increase in HF from 488 to 551 W/m^2. This change in HF can be attributed to the greater number of collisions and oscillations that occurred in response to high temperature.
- As the temperature continuously increases and reaches to 2000 K, the TC of the material increaseds from 0.26 to 0.32 W/m·K.
- Increasing the Press from 1 to 5 bar led to a corresponding increase in HF from 488 to 496 W/m^2. This change in HF can be attributed to the number of oscillations and, thus, the mobility of the structures.
- An increase in EHF from 1 to 5 W/m^2 led to a corresponding increase in HF from 503 to 538 W/m^2. This change in HF can be attributed to a corresponding increase in the number of reactions occurring in the studied structure.
- With the continuous increase of Press and reaching to 5 bar, the TC of the material increases and reveales a transition from 0.26 to 0.28 W/m·K.
- By continuous increase of EHF and reaching 5 W/m^2, TC of the material increases and reveales a transition from 0.28 to 0.31 W/m·K.

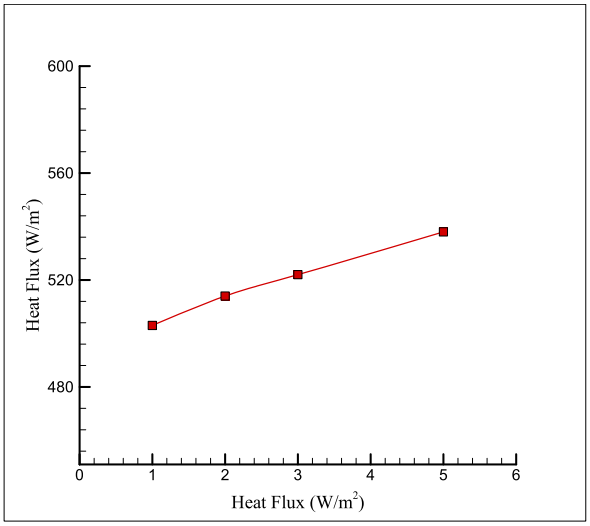

Fig. 8. The changes in HF vs EHF with 10% platinum catalyst.

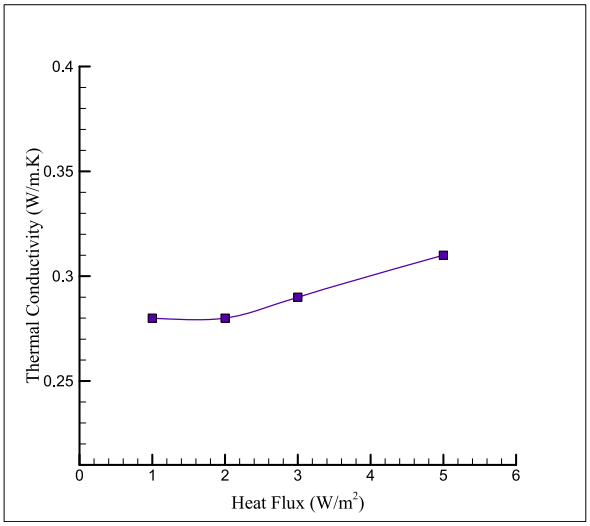

Fig. 9. The changes in TC per EHF in the presence of a 10% platinum catalyst.

Author statement

Gongxing Yan: Methodology, Software and Validation, Investigation, Revision. Omar S. Mahdy: Methodology, Software and Validation, Investigation, Revision. As'ad Alizadeh: Methodology, Software and Validation, Writing - Original Draft, Investigation. Navid Nasajpour-Esfahani: Methodology, Software and Validation, Writing - Original Draft, Investigation. Shadi Esmaeili: Methodology, Software and Validation, Writing - Original Draft, Investigation. Maboud Hekmatifar: Methodology, Software and Validation, Writing - Original Draft, Investigation. Mohamed R. El-Sharkawy: Methodology, Software and Validation, Investigation, Revision. Ahmed Salah Al-Shat: Methodology, Software and Validation, Investigation, Revision. Mahmoud Shamsborhan: Methodology, Software and Validation, Writing - Original Draft, Investigation.

Declaration of competing interest

The authors declare that they have no known competing financial interests or personal relationships that could have appeared to influence the work reported in this paper.

Data availability

No data was used for the research described in the article.

Acknowledgment

This work was supported by Sichuan Province Luzhou city of science and technology planning project(2022-GYF-16),Scientific research and innovation team construction project of Luzhou vocational and Technical College (2021YJTD07).

References

[1] F. Teymouri, Ammonia Fiber Explosion (AFEX) Treatment of Corn Stover and Effects of AFEX Treatment on Plant-Produced Heterologous Cellulase, Michigan State University, 2003.
[2] J. Goldemberg, Ethanol Sustain. Energy Future 315 (5813) (2007) 808–810.
[3] A. Demirbas, Biofuels Securing The Planet's Future Energy Needs 50 (9) (2009) 2239–2249.
[4] P. Binod, R. Sindhu, R.R. Singhania, S. Vikram, L. Devi, S. Nagalakshmi, N. Kurien, R.K. Sukumaran, A. Pandey, Bioethanol Production from Rice Straw: an Overview, vol. 101, 2010, pp. 4767–4774, 13.
[5] Y. Kim, Metabolic Engineering of Escherichia coli for Ethanol Production without Foreign Genes, 2007.
[6] Y.M. Liu, et al., Promoting electrochemical reduction of CO2 to ethanol by B/N-doped sp(3)/sp(2) nanocarbon electrode, CHINESE CHEMICAL LETTERS 33 (10) (2022) 4691–4694.
[7] H.F. Fu, et al., Enhanced ethanol sensing performance of N-doped ZnO derived from ZIF-8. CHINESE CHEMICAL, LETTERS 34 (2) (2022).
[8] X.Q. Shen, et al., Highly selective conversion of methane to ethanol over $CuFe_2O_4$-carbon nanotube catalysts at low temperature, CHINESE CHEMICAL LETTERS 33 (1) (2022) 390–393.
[9] H. Zabed, J. Sahu, A. Suely, A. Boyce, G. Faruq, Bioethanol Production from Renewable Sources: Current Perspectives and Technological Progress, vol. 71, 2017, pp. 475–501.
[10] A. Demirbas, Producing And Using Bioethanol As An Automotive Fuel 2 (4) (2007) 391–401.
[11] C. Ibeto, A. Ofoefule, K. Agbo, A global overview of biomass potentials for bioethanol production, A Renewable Alternative Fuel 6 (5) (2011) 410.
[12] S. Prasad, A. Singh, H. Joshi, Ethanol as an alternative fuel from agricultural, Industrial And Urban Residues 50 (1) (2007) 1–39.
[13] H. Li, G. Li, L. Li, J. Wu, Z. Yao, T. Zhang, Combustion characteristics and concentration measurement of ADN-based liquid propellant with electrical ignition method in a combustion chamber, Fuel 344 (2023) 128142.
[14] H. Li, G. Li, L. Li, Comparative investigation on combustion characteristics of ADN-based liquid propellants in inert gas and oxidizing gas atmospheres with resistive ignition method, Fuel 334 (2023) 126742.
[15] L. Liu, Y. Tang, D. Liu, Investigation of future low-carbon and zero-carbon fuels for marine engines from the view of thermal efficiency, Energy Reports 8 (2022) 6150–6160.
[16] L. Liu, Q. Mei, W. Jia, A flexible diesel spray model for advanced injection strategy, Fuel 314 (2022) 122784.
[17] C. Du, N. Nasajpour-Esfahani, M. Hekmatifar, D. Toghraie, S. Esmaeili, The Effect of Initial Temperature and External Heat Flux on the H2 and CO Production by Biomass Gasification Using Molecular Dynamics Simulation, 2023, 119011.
[18] E.E. Ozbas, D. Aksu, A. Ongen, M.A. Aydin, H.K. Ozcan, Hydrogen Production via Biomass Gasification, and Modeling by Supervised Machine Learning Algorithms, vol. 44, 2019, pp. 17260–17268, 32.
[19] B.J. Alder, T.E. Wainwright, Studies in molecular dynamics. I, General Method 31 (2) (1959) 459–466.
[20] N. Al-Esawi, M. Al Qubeissi, R. Kolodnytska, The Impact Of Biodiesel Fuel On Ethanol/Diesel Blends 12 (9) (2019) 1804.
[21] Y. Çelebi, H. Aydın, Investigation of the effects of butanol addition on safflower biodiesel usage as fuel in a generator diesel engine, Fuel 222 (2018) 385–393, 2018/06/15/.
[22] D.H. Qi, H. Chen, L.M. Geng, Y.Z. Bian, X.C. Ren, Performance and combustion characteristics of biodiesel–diesel–methanol blend fuelled engine, Appl. Energy 87 (5) (2010) 1679–1686, 2010/05/01/.
[23] H. An, W.M. Yang, S.K. Chou, K.J. Chua, Combustion and emissions characteristics of diesel engine fueled by biodiesel at partial load conditions, Appl. Energy 99 (2012) 363–371, 2012/11/01/.
[24] D.C. Rapaport, The Art of Molecular Dynamics Simulation, Cambridge university Press, 2004.
[25] D.C. Rapaport, D.C.R. Rapaport, The Art of Molecular Dynamics Simulation, Cambridge university Press, 2004.
[26] W.C. Swope, H.C. Andersen, P.H. Berens, K.R. Wilson, A computer simulation method for the calculation of equilibrium constants for the formation of physical clusters of molecules: application to small water clusters, J. Chem. Phys. 76 (1) (1982) 637–649.
[27] E. Hairer, C. Lubich, G. Wanner, Geometric numerical integration illustrated by the Störmer–Verlet method, Acta Numer. 12 (2003) 399–450.
[28] M.S. Daw, M.I. Baskes, Embedded-atom method: derivation and application to impurities, surfaces, and other defects in metals, Phys. Rev. B 29 (12) (1984) 6443.
[29] J.E. Lennard-Jones, Cohesion, Proc. Phys. Soc. 43 (5) (1931) 461, 1926-1948.
[30] P.G. Huray, Maxwell's Equations, John Wiley & Sons, 2011.
[31] A.K. Rappé, C.J. Casewit, K. Colwell, W.A. Goddard III, W.M. Skiff, UFF, a full periodic table force field for molecular mechanics and molecular dynamics simulations, J. Am. Chem. Soc. 114 (25) (1992) 10024–10035.
[32] H. Berendsen, J. Grigera, T. Straatsma, The missing term in effective pair potentials, J. Phys. Chem. 91 (24) (1987) 6269–6271.
[33] D. Toghraie, A.R. Azimian, Molecular dynamics simulation of annular flow boiling with the modified Lennard-Jones potential function, Heat Mass Tran. 48 (1) (2012) 141–152.
[34] M. Rezaei, A.R. Azimian, D. Toghraie, Molecular dynamics study of an electro-kinetic fluid transport in a charged nanochannel based on the role of the stern layer, Phys. Stat. Mech. Appl. 426 (2015) 25–34.
[35] S.R. Yan, et al., Prediction of boiling flow characteristics in rough and smooth microchannels using molecular dynamics simulation: investigation the effects of boundary wall temperatures, J. Mol. Liq. 306 (2020), 112937.
[36] D. Toghraie, M. Hekmatifar, Y. Salehipour, M. Afrand, Molecular dynamics simulation of Couette and Poiseuille Water-Copper nanofluid flows in rough and smooth nanochannels with different roughness configurations, Chem. Phys. 527 (2019), 110505.